

An Evaluation of the National Meteorological Center Weekly Hindcast  
of Upper-Ocean Temperature Along the Eastern Pacific Equator in January 1992

David Halpern<sup>1</sup> and Ming Ji<sup>2</sup>

<sup>1</sup> Earth and Space Sciences Division

Jet Propulsion Laboratory

California Institute of Technology

Pasadena, CA 91109

<sup>2</sup> Coupled Model Project

National Meteorological Center

National Oceanic and Atmospheric Administration

Washington, DC 20233

## ABSTRACT

The upper-ocean temperature distribution along the Pacific equator from 139 to 103°W was observed in January 1992 with temperature profiles recorded from a ship and inferred from an ocean general circulation model calculation involving data assimilation (*i. e.*, hindcast). An El Niño episode was in progress. The 100-m thick mixed layer depth, the mixed-layer temperature, and the depth-averaged temperature below the thermocline were similar in both data products. Considerable differences occurred in the representation of the 15 - 25 °C thermocline, such as the depth-averaged temperatures above and below the 20 °C isotherm, east-west slope of the 20 °C isotherm, and a 1000-km wide depression. The longitudinal-averaged root-mean-square difference between the hindcast and observed depths of the center of the thermocline was 17 m. Most of the disparities could be attributed to a high wave number transient event which the model-based assimilation system was not intended to resolve.

### 1. Introduction

The interannual El Niño warming of the surface water of the eastern equatorial Pacific produces global atmospheric climate variations. Detailed analysis of the dynamics of an El Niño episode remain elusive because subsurface flow and thermal fields, especially along the eastern Pacific equator, are severely undersampled. A tenet of faith among many oceanographers is that judicious assimilation of limited in situ observations into a realistic high-resolution, time-dependent, three-dimensional ocean general circulation model (OGCM) will provide simulated oceanographic data products suitable for dynamical analysis.

Since 1985 the National Oceanic and Atmospheric Administration (NOAA) National Meteorological Center (NMC) routinely produced an operational monthly hindcast of the previous month's upper-ocean thermal condition in the equatorial Pacific (Leetmaa and Ji, 1992). Hayes *et al.* (1989) demonstrated that estimation of thermocline depth at the equator needed further improvement. Since 1990, a new near-real time ocean model-based hindcast system routinely produces weekly hindcasts of Pacific Ocean thermal conditions with a delay of about 14 days (Ji

and Leetmaa, 1991; Leetmaa and Ji, 1992). Changes included new techniques of data assimilation, usage of the NMC forecast-analysis wind product instead of a wind field derived only from ship measurements, and assimilation of increased quantity of observations, such as subsurface temperature profiles recorded at moored buoys as well as from an increased number of ships. A comparison between the NMC weekly hindcast and a quasi-synoptic oceanographic survey of upper-ocean temperature along the equator between 139 and 103°W during January 1992 is the subject of this paper.

## 2. Data

The University of Southern California research vessel (R/V) *John V. Vickers* transited westward along the equator from 103 to 139°W for PACFLUX II investigations of the Joint Global Ocean Flux Studies (JGOFS) program. A model T4 expendable bathythermograph (XBT), which recorded temperature at 728 sequential times or "counts" between the surface and 460 m, was launched at integral longitudes. The XBT depth,  $z$ , corresponding to a count,  $c$ , is defined by  $z = 6.472 (c/10) - 0.00216 (c/10)^2$ , which is the empirical formulation provided by the manufacturer. However, Hanawa and Yoritaka, 1987) reported that the XBT falls through the water at a faster rate than that computed by the standard formula. Therefore, all *Vickers* XBT depths were increased by 5% because the data were compared with a hindcast which assimilated depth-corrected XBT data and fixed-depth temperatures from moored buoys.

The 103°W-XBT was launched on 27 December 1991 and the temperature profile at 139°W was recorded on 13 January 1992. The *Vickers* remained on station near 0°, 124°W for 6 days beginning 4 January. All XBT observations were intended to be transmitted on the Global Telecommunications System (GTS) and to be used in the NMC weekly hindcast. However, the XBT-to-GTS technique performed successfully only between 130° and 139°W or from 12 - 13 January. No *Vickers'* XBT data were assimilated between 130 and 103°W. Fortunately, the XBT recorder on the *Vickers* stored all the XBT data measured from 103 - 139°W.

The 12 - 18 January 1992 NMC hindcast temperature was created with the OGCM developed

at the NOAA Geophysical Fluid Dynamics Laboratory (GFDL) by Bryan (1969) and Cox (1984) and substantially modified for the tropical Pacific by Philander (1990). Numerous evaluations of the Philander/GFDL OGCM have proven the simulations to be reliable (Philander, 1990). The geographical domain of the NMC version of the Philander/GFDL OGCM was 120°E to 70°W and 45°S to 55°N, with sponge regions poleward of 35°S and 45°N. Within the sponge layers the model temperature and salinity fields were forced to relax to the climatological values. The 1.5° east-west resolution of the NMC hindcast was slightly greater than the 1°-longitudinal spacing of the Philander/GFDL OGCM; the 1/3° north-south resolution between 10°S and 10°N remained unchanged. Weekly-averaged hindcasts were stored on a 1°-latitude and 1.5°-longitude grid. The vertical resolution and the 1-h time step of the NMC hindcast were the same as the Philander/GFDL OGCM. There were 10 equal layers above 100 m, and we used the uppermost 19 levels, which occurred above 423 m. The NMC hindcast methodology did not alter the Richardson Number dependent vertical mixing parameterization used in the Philander/GFDL OGCM. Also, the horizontal eddy exchange coefficients ( $1 \times 10^3 \text{ m}^2 \text{ s}^{-1}$ ) were the same. The net air-sea heat flux was set to zero because SST was continuously assimilated.

A continuous data assimilation scheme, which was implemented at NMC in 1989 (Ji and Leetmaa, 1991), uses variational optimal interpolation (Derber and Rosati, 1989) to combine surface and subsurface temperature measurements with the modeled temperatures. The SST data were obtained from a variety of instrument platforms: day and night multichannel SST retrievals from NOAA polar-orbiting satellites; ships; satellite-tracked drifting buoys. Subsurface temperature measurements were recorded from moored buoys and from XBTs launched from the ship-of-opportunity network (Figure 1). The depths of all XBT temperatures were increased by 5% (Hanawa and Yoritaka, 1987).

Extensive quality control eliminated spurious subsurface temperature measurements. Each subsurface temperature profile was compared with the profile computed from the previous week hindcast and/or a climatological-mean profile at the same site to discard data considered incorrect. Approximately 2 - 5% of the weekly XBT data set were discarded. Comparison of a ship's track

determined from the locations affixed to XBT data and the ship's weather reports revealed location errors.

Data assimilation was done continuously during model integration. At an assimilation time step, all subsurface temperature observations recorded 2 weeks before and 2 weeks after this time and all SST data recorded 1 week before and 1 week after this time were assimilated. The hindcast temperature at the time step immediately prior to the assimilation time serves as the first-guess estimate. For each grid point, error covariances and temperature differences were computed between the first-guess temperature field and all data occurring within a  $4^\circ$  domain of influence. The error covariances were weighted with a Gaussian function to account for the distances between data values. An objectively analyzed temperature correction, which was computed with the error covariances and temperature differences (Lorenz, 1986) and which was weighted by the 2-week or 4-week data window (Derber and Rosati, 1989), was added to the first-guess temperature to create the optimal interpolated temperature for the next integration time step. The assimilation was made for 3 consecutive 1-h time steps every 12 h of integration time. The small modification made to the hindcast on all the 1-h integration time steps allows the circulation to adjust to the thermal field almost instantaneously.

A 12 - 18 January weekly-averaged surface wind stress distribution, which was centered at 1200 GMT on Wednesday 15 January, was computed from the 6-hourly NMC global atmospheric forecast-analysis system. The weekly-averaged wind stress was linearly interpolated at 1-h intervals to match the hindcast integration time step.

### **3. Results**

The XBT surface temperatures at 110, 124, 139, and  $140^\circ\text{W}$  on 28 December and 10, 13 and 19 January, respectively, were virtually identical to 1-m depth daily-averaged measurements recorded at moored buoys at 110, 125 and  $140^\circ\text{W}$  (Freitag and McPhaden, 1992; Hayes, 1992).

The observed XBT temperature section (Figure 2A) was gridded to conform to the depths and longitudes of the NMC hindcast. A 1-m averaged XBT temperature centered at the middle

depth of each OGCM layer was computed. We intentionally did not compute the average XBT temperatures within the depth intervals corresponding to the hindcast layers because the objective is to determine the hindcast representativeness of the natural state. Temperature at the hindcast 1.5°-longitudinal interval was linearly interpolated from the XBT data adjacent to the hindcast longitudes. A less intense vertical gradient of temperature occurs in the thermocline of the gridded XBT data (Figure 2B). The 100-m thick near-surface mixed layer and the 100-m thick 13 °C thermostad (defined as the 12 - 14 °C depth interval) were independent of the depth-longitude grid resolution.

The 12 - 18 January weekly NMC hindcast of the upper-ocean temperature distribution (Figure 2C), which was computed with assimilation of the 12 - 13 January *Vickers* XBT data from 130 - 139°W, resembled the gridded XBT observations (Figure 2B). The hindcast (Figure 2C) was very similar to the corresponding hindcast (not shown) computed without assimilating any *Vickers* XBT data: all grid-point differences were smaller than 0.5 °C except between 25 and 75 m from 133 to 138°W where the differences were less than 1.0 °C. Assimilation of 139 - 130°W *Vickers* XBT data had almost no effect upon the NMC hindcast thermocline.

Throughout the 139 - 103°W interval the XBT and hindcast temperatures (Figures 2B and 2C) within the uppermost 100 m and from 200 - 363 m were especially similar (Figures 2D). Larger differences occurred within the thermocline between 100 and 200 m depths (Figures 2D). The grid-point maximum absolute-value temperature difference was 6.3 °C at 136 m at 114°W, where the depth-averaged 100 - 150 m hindcast temperature was 5 °C less than that observed (Figure 2E).

Between 139 and 120°W the hindcast produced higher temperatures in the thermocline (Figure 2D). This phenomenon may be explained by an upwelling transient event which was not resolved by the hindcast-analysis system. An upwelling event was recorded at the moored buoys at 2°S and 2°N along 140°W on about 10 January.

Between 120 and 110°W the hindcast temperatures in the upper portion of the thermocline were substantially lower (Figure 2D). At 114°W the observed 150-m depth of the 20 °C isotherm,

which occurs in the middle of the equatorial thermocline (Colin *et al.*, 1971; Halpern, 1987) and which is considered representative of the depth of the thermocline, was 35 m deeper than in the hindcast (Figure 2F).

A possible cause of the 120 - 110°W downward displacement of the measured thermocline is eastward propagation of a downwelling Kelvin wave. Evidence was found in the 0°, 155°W and 0°, 125°W moored-buoy measurements of the depth of the 20 °C isotherm (Hayes, 1992) that from 2 to 17 December a 25-m downwelling disturbance in the thermocline moved eastward from 155 to 125°W at about 2.5 m s<sup>-1</sup> (*i. e.*, about 2° longitude per day), which corresponded to the propagation speed of a first-mode baroclinic Kelvin wave (Knox and Halpern, 1982). Inspection of Dr. Michael McPhaden's (personal communication, 1992) daily-averaged Equatorial Undercurrent (EUC) transports per unit latitudinal width at 0°, 140°W and 0°, 110°W revealed that the maximum EUC transport during 10 November to 20 January occurred at 140°W on 4 December and at 110°W on 21 December; thus, the eastward speed of the maximum EUC transport was 2.2 m s<sup>-1</sup>. The thermocline depression was also observed on 22 November at 0°, 170°W (Hayes, 1992) and traveled to 0°, 155°W at 2.0 m s<sup>-1</sup>. Had the thermocline depression at 125°W continued eastward at 2.5 m s<sup>-1</sup>, then the maximum depth of the feature would have passed 114°W on about 22 December, which was nearly 12 days before the Vickers XBT measurement was made at 114°W, and would have reached the Galápagos Archipelago on 3 January. Examination of Professor Klaus Wyrki's (personal communication, 1992) sea level measurements at Baltra (0°, 90°W) indicated a nearly monotonic 15-cm rise from 21 December to 1 January. Baltra sea surface heights were nearly uniform from 3 - 8 January and then experienced a rapid 10-cm rise reaching a maximum for the month on 13 January, which was 10 days after the maximum depression passed 114°W. The time interval for a Kelvin wave pulse moving at 2.5 m s<sup>-1</sup> to travel from 114°W to Baltra would be about 12 days, which was nearly the same as the 10-day observed time separation. A sea level variation similar to the one at Baltra was subsequently observed along the coast of Peru (Enfield, 1992). An increase in sea surface height corresponds to a thermocline depression because the increased quantity of heat stored above the thermocline produces higher sea surface

height. The *Vickers* data combined with the Hayes (1992) and Wyrki (personal communication, 1992) measurements suggest the occurrence of a Kelvin wave pulse from 170 to 155°W, 155 to 125°W, and 114 to 90°W. That the travel time between 125 and 114°W was not consistent with the Kelvin wave evidence is an enigma. Did the Kelvin wave speed decrease in the eastern Pacific, such as observed during the 1987 El Niño by Halpern and Zlotnicki (1992), or were there more than one Kelvin wave pulse are questions beyond the scope of this report.

The 139 - 103°W longitudinal-averaged hindcast and observed depths of the 20 °C isotherm were different by 5 m. The two curves in Figure 2F were not linearly correlated because the correlation coefficient was less than 0.1 and not statistically significant at the 95% level. That the 17-m root-mean-square (rms) difference was three times larger than the mean difference means large differences occurred (Figure 2F). The longitudinal-averaged rms difference was similar to the 1985 - 1987 average rms difference at 140 and 110°W (Hayes *et al.*, 1989), which does not indicate a dramatic improvement in the hindcast depth of the center of the thermocline.

Tidal internal gravity wave motions produce vertical displacements of the depth of the 20 °C isotherm (and all isotherms), which create an uncertainty in the interpretation of XBT measurements. Two time series of the depth of the 20 °C isotherm were computed at 0°, 110°W where conductivity-temperature-depth (CTD) measurements were recorded at 2-h interval for 48 h on 9 - 11 February 1979 and at 1-h interval for 12 h on 4 May 1979 (Mangum *et al.*, 1980). For each time series the standard deviation of the vertical displacements of the 20 °C isotherm was 4 m. A similar estimate of 20 °C isotherm displacement was determined at 0°, 140°W from the Chereskin *et al.* (1986) intensively sampled 12-day time series. If a normal distribution of isotherm depth fluctuations is assumed, then twice the standard deviation represents the reliability within 95% confidence limits of the depth of the 20 °C isotherm. Thus, the XBT and hindcast depths of the 20 °C isotherm (Figure 2F) were statistically different at the 95% confidence level throughout most of the 139 - 103°W region.



#### 4. Discussion

The 12 - 18 January 1992 NMC weekly-averaged hindcast of temperature along the equator in the eastern Pacific was compared with XBT observations during the anomalous ocean-atmosphere interactions associated with the 1991 - 1992 El Niño. The XBT and hindcast temperatures and depths of the mixed layer were almost identical. Similarly, the 13 °C thermostat was in excellent agreement.

The most substantial differences between the *Vickers* data and the hindcast occurred within the thermocline. Both the absence of the 9°-wide depression centered near 115°W and the greater upward slope towards the east from 139 - 115°W in the hindcast may be caused by a combination of inadequate surface wind and the effects of the assimilation scheme, which are described below. The influence of approximate 20-day period, 1000-km zonal wave length current and temperature oscillations (Halpern *et al.*, 1988) is considered to be negligible because the amplitude of the wave motion is greatly reduced during an El Niño episode.

The surface wind field in the narrow equatorial wave guide is very important to simulate thermal and flow fields along the equator (McCreary, 1976). For instance, a 15% smaller westward wind stress leads to a deepening of the hindcast thermocline, which increases from 5 m at 140°W to 25 m at 105°W (Leetmaa and Ji, 1989). In March 1991, NMC introduced the T126 version of the atmospheric general circulation model forecast-analysis system. The new NMC-derived equatorial Pacific surface wind field remains to be evaluated.

Another important factor contributing to the differences between the *Vickers* XBT and NMC hindcast data sets is the data assimilation technique. The 4°-radius of influence and 4-week subsurface data window was designed to filter fluctuations with submonthly time scales. The moored-buoy measurements had a greater impact upon the hindcast in the narrow equatorial zone compared to XBT data because moored measurements were recorded continuously with time unlike the sporadic XBT sampling. Inspection of Figure 1 indicates that in the  $\pm 2^\circ$ -latitudinal equatorial radius of deformation (Gill, 1982) between 140 and 103°W the only subsurface temperature observations during January were the few XBTs from the *Vickers* and the continuous

moored-buoy measurements at 140, 125, and 110°W. The time window for assimilation of moored-buoy data could be reduced for a weekly-averaged hindcast, which would not diminish the quantity of data because the moored-buoy measurements are recorded continuously. The hindcast would then be expected to yield a more accurate representation of the transient thermocline depression. It remains to be tested whether the spatial sampling resolution for oceanographic data assimilated into an OGCM need be as high as that described by the Nyquist Theorem.

*Acknowledgements.* We are indebted to Professor Richard Dugdale (USC), who informed DH in November 1991 of the forthcoming R/V *Vickers* voyage in December, Paul Stevens (NOAA), who kindly and rapidly provided the XBTs and arranged for their shipment to the R/V *Vickers*, Captain Kurt Schnebele (NOAA) and the R/V *Vickers* crew, who launched the XBTs and recorded the necessary auxiliary information, and Steven Cook (NOAA), who instructed the R/V *Vickers* crew on the operation of the XBT system. Professor Douglas Hammond (USC), who was the R/V *Vickers* Chief Scientist, and Donald Newman (USC) contributed towards the successful acquisition of the XBT measurements. William Knauss (JPL) processed the XBT and hindcast data and prepared graphical and tabular analyses in his usual outstanding manner. Patrick Caldwell (University of Hawaii) kindly dispatched the Baltra sea level measurements, which is maintained under the direction of Professor Klaus Wyrtki (University of Hawaii). The moored-buoy subsurface temperature measurement array, which is maintained under the direction of Dr. Stanley Hayes (NOAA), was valuable. Dr. Michael McPhaden (NOAA) kindly computed the EUC transports per unit width from PROTEUS measurements. Linda Mangum (NOAA) and Linda Stratton (NOAA) maintained a weekly transfer of moored-bouy temperature data from the Pacific Marine Environmental Laboratory to NMC. Helpful discussions with Dr. Yi Chao (UCLA), Dr. Mojib Latif (MPI), and Dr. Ants Leetmaa (NOAA) improved an early version of the manuscript. Data analysis was supported by NASA RTOP No. 578-22-26 (DH). The research was carried out, in part, by the Jet Propulsion Laboratory, California Institute of Technology, under a contract with the National Aeronautics and Space Administration.

## REFERENCES

- Bryan, K., 1969: A numerical method for the study of the world ocean. *Journal of Computational Physics*, 4, 347-376.
- Chereskin, T.K., J.N. Moum, P.J. Stabeno, D.R. Caldwell, C.A. Paulson, L.A. Regier and D. Halpern, 1986: Fine-scale variability at 140°W in the equatorial Pacific. *Journal of Geophysical Research*, 91, 12887-12897.
- Colin, C., C. Henin, P. Hisard and C. Oudot, 1971: Le courant de Cromwell dans le Pacifique central en Février 1970. *Cahiers O. R. S. T. O. M., Serial Oceanographie*, 9, 167-186.
- Cox, M.D., 1984: A primitive, 3-dimensional model of the ocean. GFDL Ocean Group Technical Report No. 1, Geophysical Fluid Dynamics Laboratory, 143 pp.
- Derber, J. and A. Rosati, 1989: A global oceanic data assimilation system. *Journal of Physical Oceanography*, 19, 1333-1347.
- Enfield, D., 1992: Figure T33. In: *Climate Diagnostics Bulletin, January 1992*, No. 92/1, National Oceanic and Atmospheric Administration, 34.
- Freitag, H.P. and M. McPhaden, 1992: Figure T30. In: *Climate Diagnostics Bulletin, January 1992*, No. 92/1, National Oceanic and Atmospheric Administration, 31.
- Gill, A.E., 1982: *Atmosphere-Ocean Dynamics*. Academic Press, 662 pp.
- Halpern, D., 1987: Observations of annual and El Niño thermal and flow variations along the equator at 0°, 110°W and 0°, 95°W During 1980 - 1985. *Journal of Geophysical Research*, 92, 8197-8212.
- Halpern, D. and Zlotnicki, 1992: Observations of a Pacific equatorial Kelvin wave pulse in January 1987 with GEOSAT altimetric data. In: *Proceedings of the Conference: Oceans From Space, Venice 1990*, editor, J.R. Apel, International Association of the Physical Sciences of the Ocean, Del Mar, CA, in press.
- Halpern, D., R.A. Knox and D.S. Luther, 1988: Observations of 20-day period meridional current oscillations in the upper ocean along the Pacific equator. *Journal of Physical Oceanography*, 18, 1514-1534.

- Hanawa, K. and H. Yoritaka, 1987: Detection of systematic errors in XBT data and their correction. *Journal of the Oceanographical Society of Japan*, 43, 68-76.
- Hayes, S.P., M. McPhaden and A. Leetmaa, 1989: Observational verification of a quasi real time simulation of the tropical Pacific Ocean. *Journal of Geophysical Research*, 94, 2147-2157.
- Hayes, S.P., L.J. Mangum, J. Picaut, A. Sumi and K. Takeuchi, 1991: TOGA-TAO: A moored array for real-time measurements in the tropical Pacific Ocean. *Bulletin of the American Meteorological Society*, 72, 339-347.
- Hayes, S.P., 1992: Figure T31. In: *Climate Diagnostics Bulletin, January 1992*, No. 92/1, National Oceanic and Atmospheric Administration, 32.
- Ji, M. and A. Leetmaa, 1991: An ocean observing system for seasonal prediction using coupled models. In: *Papers Presented at the Joint IOC/WMO Seminar on IGOSS Products, Tokyo, 15-19 April 1991*, World Meteorological Organization, 315-326.
- Knox, R. A. and D. Halpern, 1982: Long range Kelvin wave propagation of transport variations in Pacific Ocean equatorial currents. *Journal of Marine Research*, 40 Supplement, 329-339.
- Leetmaa, A. and M. Ji, 1989: Operational hindcasting of the tropical Pacific. *Dynamics of Atmospheres and Oceans*, 13, 465-490.
- Leetmaa, A. and M. Ji, 1992: Figure T15. In: *Climate Diagnostics Bulletin, January 1992*, No. 92/1, National Oceanic and Atmospheric Administration, 16.
- Lorenc, A.C., 1986: Analysis methods for numerical weather prediction. *Quarterly Journal of the Royal Meteorological Society*, 112, 1117-1194.
- Mangum, L.J., N.N. Soreide, B.D. Davies, B.D. Spell and S.P. Hayes, 1980: CTD/O<sub>2</sub> measurements during the Equatorial Pacific Ocean Climate Study (EPOCS) in 1979. NOAA Data Report ERL PMEL-1, Pacific Marine Environmental Laboratory, 645 pp.
- McCreary, J., 1976: Eastern tropical ocean response to changing wind systems: With application to El Niño. *Journal of Physical Oceanography*, 6, 632-645.
- Philander, S.G., 1990: *El Niño, La Niña, and the Southern Oscillation*. Academic Press, 289 pp.

## List of Figures

Figure 1. Locations of temperature profiles used in the preparation of the 12 - 18 January 1992 hindcast. A total of 2321 temperature profiles (983 from XBTs and 1338 from moored buoys) were assimilated in January 1992 to produce the weekly-averaged hindcast centered on 15 January. Small dots represent XBT observations from the ship-of-opportunity network. Triangles represent moored-buoy sites, which are described by Hayes *et al.* (1991).

Figure 2. Upper-ocean temperature distribution ( $^{\circ}\text{C}$ ; contour interval is  $1^{\circ}\text{C}$ ) along the equator: (A) XBT measurements recorded from the R/V *Vickers* during 27 December 1991 - 13 January 1992; (B) XBT measurements to conform with hindcast grid; (C) 12 - 18 January NMC weekly-averaged hindcast with assimilation of R/V *Vickers* XBT data recorded from  $139^{\circ}\text{W}$  to  $130^{\circ}\text{W}$ . (D) Grid-point temperature differences ( $^{\circ}\text{C}$ ; contour interval is  $0.5^{\circ}\text{C}$ ) between gridded XBT data, (B), and NMC hindcast, (C). (E) Longitudinal distributions of depth-average temperature over a variety of depth intervals, which were computed from the gridded XBT measurements, (B) and the NMC hindcast, (C). Dashed line represents gridded XBT data; solid line represents NMC hindcast. (F) Longitudinal distributions of the depths of the  $20^{\circ}\text{C}$  isotherm. Dashed line represents gridded XBT data, (B); solid line represents NMC hindcast, (C).

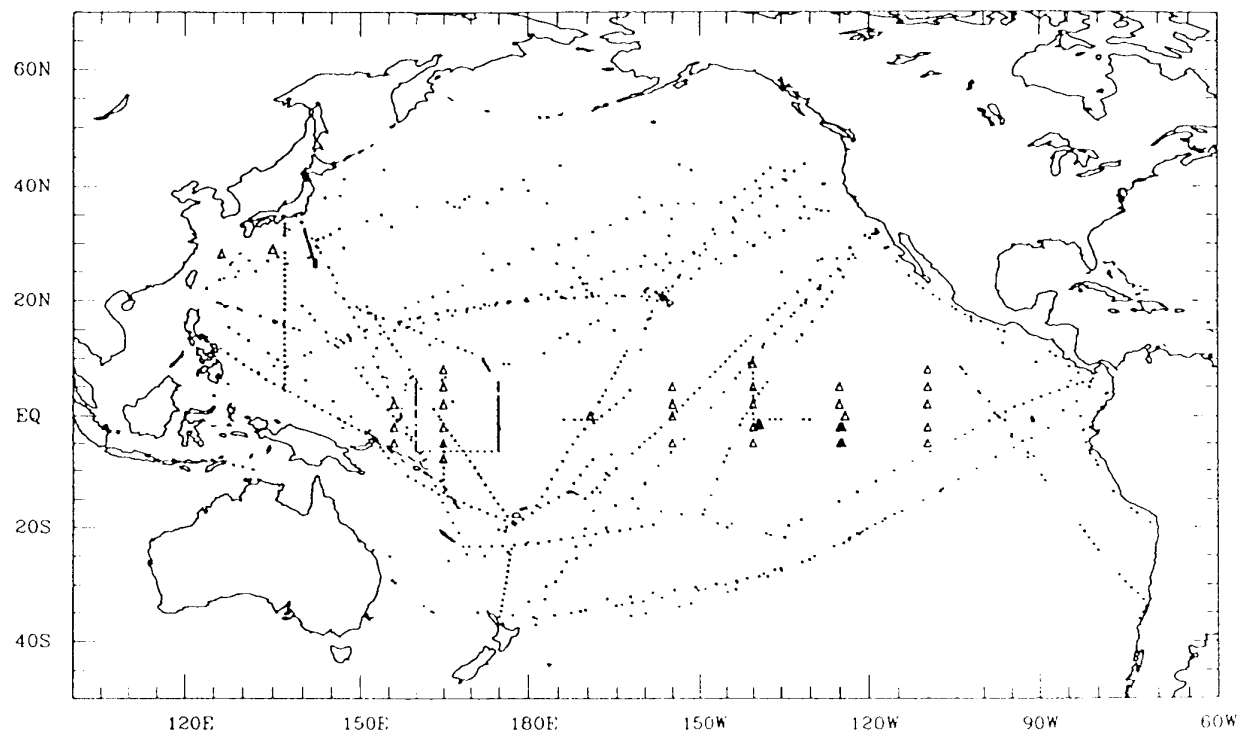


Figure 1

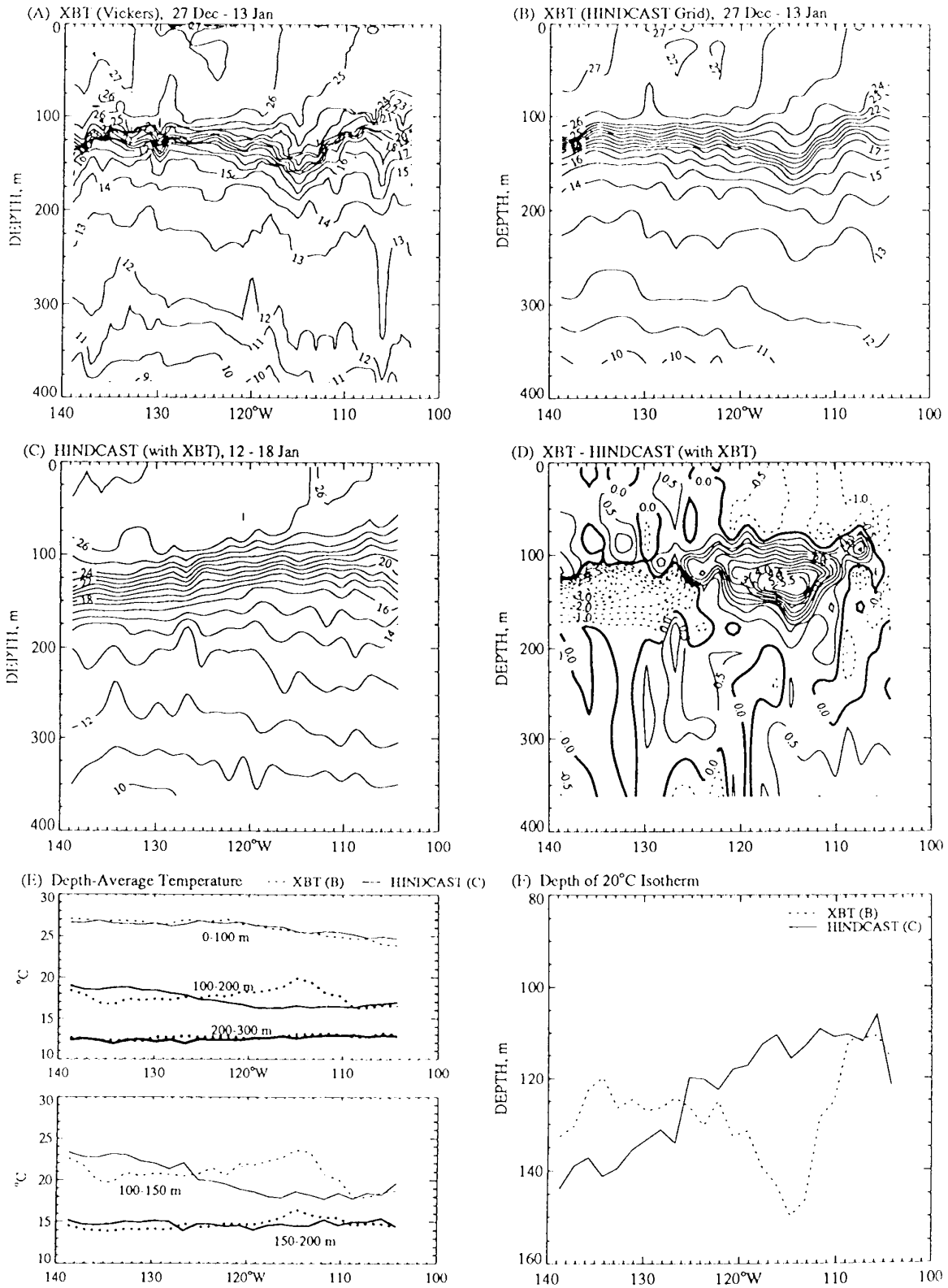


Figure 2